Astrophys Space Sci (2018) 363:12
https://doi.org/10.1007/s10509-017-3232-7

ORIGINAL ARTICLE

Deuterium chemistry in the young massive protostellar core NGC 2264 CMM3

Z. Awad[1] · O.M. Shalabiea[1]

Received: 4 July 2017 / Accepted: 7 December 2017 / Published online: 14 December 2017

Abstract In this work we present the first attempt of modelling the deuterium chemistry in the massive young protostellar core NGC 2264 CMM3. We investigated the sensitivity of this chemistry to the physical conditions in its surrounding environment. The results showed that deuteration, in the protostellar gas, is affected by variations in the core density, the amount of gas depletion onto grain surfaces, the CR ionisation rate, but it is insensitive to variations in the H_2 ortho-to-para ratio.

Our results, also, showed that deuteration is often enhanced in less-dense, partially depleted ($< 85\%$), or cores that are exerted to high CR ionisation rates ($\geq 6.5 \times 10^{-17}$ s^{-1}). However, in NGC 2264 CMM3, decreasing the amount of gas depleted onto grains and enhancing the CR ionisation rate are often overestimating the observed values in the core. The best fit time to observations occurs around (1–5) $\times 10^4$ yrs for core densities in the range (1–5) $\times 10^6$ cm^{-3} with CR ionisation rate between (1.7–6.5) $\times 10^{-17}$ s^{-1}. These values are in agreement with the results of the most recent theoretical chemical model of CMM3, and the time range of best fit is, also, in-line with the estimated age of young protostellar objects.

We conclude that deuterium chemistry in protostellar cores is: (i) sensitive to variations in the physical conditions in its environment, (ii) insensitive to changes in the H_2 ortho-to-para ratio. We also conclude that the core NGC 2264 CMM3 is in its early stages of chemical evolution with an estimated age of (1–5) $\times 10^4$ yrs.

✉ Z. Awad
zma@sci.cu.edu.eg

O.M. Shalabiea
shalabiea@sci.cu.edu.eg

[1] Astronomy, Space Science and Meteorology Department, Faculty of Science, Cairo University, Giza, Egypt

Keywords Astrochemistry · Stars: massive, protostars, formation · ISM: abundances, molecules

1 Introduction

Although the standard interstellar atomic deuterium-to-hydrogen ratio (D/H ratio) is low ($\sim 10^{-5}$; Oliveira et al. 2003), observations revealed that this ratio is increased in several astrophysical regions by few orders of magnitudes (e.g. Tiné et al. 2000; Ceccarelli et al. 2001, 2007; Loinard et al. 2001; Crapsi et al. 2005; Sakai et al. 2007; Coutens et al. 2013; Vastel et al. 2017). This phenomena is known as super-deuteration (D/H $> 10\%$). It is obtained for some species such as H_2CO and CH_3OH in low-mass protostars (e.g. Ceccarelli et al. 2007 and references therein). To-date, more than 30 deuterated species have been observed in different astrophysical regions with abundances comparable, sometimes, to their normal hydrogen counterparts (also known as main isotope). These species are ranged from singly (e.g. HD, H_2D^+, DCO^+, CH_2DOH, HDO, NH_2D, $DCOOCH_3$) to multiply[1] deuterated species (e.g. D_2H^+, D_2CO, CHD_2OH, CD_3OH, NHD_2, ND_3). Details on observations of deuterated species in different astrophysical regions can be found in reviews such as Herbst and van Dishoeck (2009), Caselli and Ceccarelli (2012), Tielens (2013). Also, a list of most of the observed deuterated species in cores in massive and low-mass star forming regions is given in Table 1 in Awad et al. (2014) while Table 19 in Albertsson et al. (2013) summarises the molecular D/H ratios in different interstellar environments.

[1] **Singly (or mono-) deuterated:** are species in which only one hydrogen atom is replaced by a deuterium while **multiply deuterated:** are species in which two or more hydrogen atoms are replaced.

In the last few decades, numerous models were published to study the deuterium chemistry in the interstellar medium (ISM). Early attempts of modelling deuterium chemistry relayed on either pure gas-phase (Watson 1980) or surface chemistry (Tielens 1983). Brown and Millar (1989a,b) introduced the first gas-grain chemical model to study deuterium chemistry in dense regions. After that, Millar et al. (1989) published a model of a particular importance because its results highlighted the temperature dependence of the main source of deuterium fractionation.[2] These findings showed that in cold regions ($T \sim 10$ K) H_2D^+ and its daughter ions DCO^+ and H_2DO^+ led to high fractionation while in warmer regions ($10 < T(\mathrm{K}) < 70$) sources of high deuteration are CH_2D^+, C_2HD^+, and associated species. Years after, Rodgers and Millar (1996) gave the first recipe to extend a given gas-phase chemical network to include deuterated species by assuming that hydrogenated and their deuterated counterparts react with the same rate coefficients. More recently, Aikawa et al. (2012) published another method for extending chemical networks in which they rely on statistical probabilities in determining the rate of a deuterated reaction from its original rate of reaction. Both recipes have been used in several studies (e.g. Roberts and Millar 2000a,b; Roberts et al. 2003, 2004; Flower et al. 2006; Sipilä et al. 2010; Albertsson et al. 2013; Coutens et al. 2013, 2014; Awad et al. 2014; Hincelin et al. 2014; Furuya et al. 2016; Majumdar et al. 2017). The effect of including the spin state (ortho, para, and meta) of species on the deuterium fractionation in cold environments was also studied and it is found to influence the fractionation (e.g. Gerlich et al. 2002; Walmsley et al. 2004; Flower et al. 2006; Sipilä et al. 2010; Hincelin et al. 2014).

The massive cluster-forming region NGC 2264 was a target of several recent studied to investigate its dynamics and morphology (e.g. Peretto et al. 2006, 2007; Maury et al. 2009; Saruwatari et al. 2011) and chemistry (Watanabe et al. 2015). The analysis of the spectral survey by Watanabe et al. (2015) identified about 36 species in the young massive protostellar core NGC 2264 CMM3 among which seven deuterated species were detected. These species are DCO^+, N_2D^+, DCN, DNC, CCD, HDCO, and DC_3N. All of these molecules have been detected, separately, in dark clouds (Loren and Wootten 1985; van der Tak et al. 2009), prestellar cores and protoplanetary disks (Miettinen et al. 2012; van Dishoeck et al. 2003; Öberg et al. 2015; Huang and Öberg 2015; van der Tak et al. 2009), and in star-forming regions (van Dishoeck et al. 1995; Sakai et al. 2009; Bergman et al. 2011). In CMM3, neither singly deuterated methanol nor multiply deuterated species were reported (Watanabe et al. 2015). The authors contributed this non-detection to the limitation and insufficient sensitivity of their millimetre line survey (~ 30 mK at the corresponding frequency of CH_2DOH; Watanabe et al. 2015).

The most recent observations by Watanabe et al. (2015) motivated Awad and Shalabeia (2017) to introduce the first gas-grain astrochemical model of CMM3 that looked into the chemical evolution of a selected set of these species that do not include deuterium. The identification of few deuterated species in CMM3 motivated us to modify this model and update its chemical network to include all possible deuterated species in order to understand their chemical evolution of in CMM3. Therefore, the main aim of this work is to investigate the sensitivity of deuterium chemistry in protostellar cores, specifically CMM3, to variations in the physical parameters namely; the density, the depletion onto grain surfaces, and the CR ionisation rate. Moreover, we examined the effect on changing the H_2 ortho-to-para ratio (OPR) on the deuterium chemistry in the protostellar phase.

This paper is organised as follows: we describe the used chemical model and the initial conditions in Sect. 2, the results are discussed in detail in Sect. 3, and finally our concluding remarks are summarised in Sect. 5.

2 Chemical models and initial conditions

The chemical model used in the present work is based on the previously published model by Awad and Shalabeia (2017) for the protostellar core NGC 2264 CMM3, but with a modified chemical network that includes all the possible forms of deuterated species of a given normal isotope. Briefly, the model used is a single point, time-dependent, gas-grain astrochemical model. CMM3 is a protostellar object hence the formation of molecules has been started before its formation. For this reason, we start following the chemistry of CMM3 after running a pre-phase under dark cloud conditions to obtain the initial input chemistry for the protostellar phase. In this pre-phase, we follow the chemistry of low-density gas (~ 400 cm^{-3}), initially atomic, undergoes a free fall collapse, following Rawlings et al. (1992), at 10 K to reach a final density 5.4×10^6 cm^{-3}, which is observed for CMM3, in 10^6 yrs. The chemistry takes place both in gas-phase and on grain surfaces with the standard values of radiation field (1 Draine) and CR ionisation rate ($\zeta_{\mathrm{ISM}} = 1.3 \times 10^{-17}$ s^{-1}). Following Rawlings et al. (1992) and Snow and McCall (2006), the visual extinction, A_v, in this phase varies as function of the gas density as

$$A_v\ (\mathrm{mag}) = \frac{\text{gas density } (\mathrm{cm}^{-3}) \times \text{core size (cm)}}{N(\mathrm{H})\ (\mathrm{cm}^{-2})}$$

where $N(\mathrm{H})$ is the standard column density of hydrogen at A_v of 1 magnitude; 1.6×10^{21} cm^{-2}. The results of the final

[2] **Fractionation** is usually defined as the ratio between the molecule XH and its deuterated counterpart XD. However, sometimes, it refers to the amount of deuterated species formed from a given pathway. The latter definition is what we use in this work.

Table 1 Initial physical conditions and chemical abundances utilized in this study for the RM of CMM3 in both Phase I, the dark cloud conditions, and Phase II, the protostellar core conditions

Physical Conditions		
Parameters	Phase I	Phase II[a]
Core density (cm^{-3})	400–5.4×10^6	5.4×10^6
Core temperature (K)	10	15
Core radius (pc)	0.04	0.03
†Depletion	full	–
††ζ (s^{-1})	1.3×10^{-17}	1.69×10^{-17}
Chemical Abundances		
Species	Phase I[b]	‡Phase II
Helium	8.50×10^{-2}	–
Carbon	2.69×10^{-4}	–
Oxygen	4.90×10^{-4}	–
Nitrogen	6.76×10^{-5}	–
‡‡HD	1.5×10^{-5}	–
CO	–	5.4×10^{-12}
N_2	–	4.2×10^{-10}
H_2D^+	–	6.6×10^{-12}
C_2HD^+	–	$< 1.0 \times 10^{-13}$
CH_2D^+	–	$< 1.0 \times 10^{-13}$

†This parameter is related to the freeze-out process occur in the core, only in the pre-phase. The gas is considered fully depleted if more than 90% of the species gas-phase abundances are involved into grain surface reactions

††Dark cloud chemistry runs under the standard CR ionisation rate, $\zeta_{ISM} = 1.3 \times 10^{-17}$ s^{-1}, while in the protostellar phase, this value is enhanced by 1.3 times (Awad and Shalabeia 2017)

‡The low values of the initial molecular abundances in Phase II is due to their depletion onto grain surfaces (see Sect. 2 and Sect. 3)

‡‡HD molecules represent the abundance of atomic D in the gas following Awad et al. (2014); given that D/H ratio = 10^{-5} (Oliveira et al. 2003)

References: (a) Peretto et al. 2006, (b) Asplund et al. 2009

time step of this pre-phase is considered as the initial input for the chemistry occurs in the protostellar phase. By the end of the prestellar phase, most of the species were frozen onto grain surfaces.

The chemistry, in the protostellar phase, is then followed in a steady core of uniform density of 5.4×10^6 cm^{-3} (Peretto et al. 2006), corresponds to a point of $A_v = 314$ mag calculated self-consistency in the code. This value is in agreement with the observed range of visual extinctions in the region NGC 2264 (Ward-Thompson et al. 2000). The core has a temperature of 15 K and is irradiated by the standard interstellar radiation field of 1 Draine, and the cosmic ray ionisation reactions occur at a rate of $\zeta_{CMM3} = 1.67 \times 10^{-17}$ s^{-1} (Awad and Shalabeia 2017). The physical conditions of CMM3 and the initial chemical elemental abundances are listed in Table 1.

Table 2 The grid of models studied in the present work. The table lists the main differences in the physical parameters compared to the reference model (RM), keeping the rest of the parameters stated in Table 1 unchanged

Model	Density (cm^{-3})	†Depletion	‡ζ_{CMM3} (ζ_{ISM} s^{-1})
RM	5.4×10^6	full	1.3
M1	1.0×10^6	full	1.3
M2	2.7×10^7	full	1.3
M3	5.4×10^6	partial	1.3
M4	5.4×10^6	none	1.3
M5	5.4×10^6	full	5
M6	5.4×10^6	full	10

†Partially depleted gas means, in this study, that ∼ 85% of the amount of the gaseous species are involved in grain surface reactions, while none-depleted gas represents the pure gas-phase chemistry in which 0% of the gas is involved in surface reactions

‡The cosmic ray ionisation rate in CMM3 in units of the standard rate; ζ_{ISM}

The chemistry takes place both in gas-phase and on grain surfaces. The gas-phase chemical network is adapted from the latest release of KIDA astrochemical database[3] for dense media (Wakelam et al. 2015). The reactions of deuterated species are generated from their normal counterparts following the methodology described in details in Aikawa et al. (2012) and Furuya et al. (2013). In addition, we have included all the multiply deuterated form of H_3^+ for their important role in deuteration (Roberts et al. 2003). We have also added the nuclear spin states of H_2, H_3^+, and their isotopologues (e.g. Flower et al. 2006; Sipilä et al. 2010; Hincelin et al. 2014; Coutens et al. 2014). We considered the statistical ortho-to-para ratio of H_2 of 3 (Coutens et al. 2014; Hincelin et al. 2014). The surface chemical network is mainly simple hydrogenation and deuteration of the depleted species, in addition to the other surface reactions described in details in Awad and Shalabeia (2017). Mantle species are returned to the gas-phase by non-thermal desorption mechanisms; H_2 formation, CR-photodissociation, and CR induced photodesorption (Roberts et al. 2007). Thermal evaporation is not efficient in such low temperature (15 K).

In addition to the reference model (*hereafter* the RM), we performed six other models (M1 to M6) to investigate how the core deuterium chemistry is affected by its surrounding physical conditions. Table 2 lists the grid of these models; giving the values of the three physical parameters we studied compared to the reference model (in the first raw). In addition to those six models, we performed few models by

[3]KIDA: KInetic Database for Astrochemistry (http://kida.obs.u-bordeaux1.fr). We used the rate file kida.uva.2014.

which we investigated the effect of varying the H_2 OPR from the statistical ratio of 3 down to 0.003, following Pagani et al. (2011) on the deuterium chemistry of the protostar. The chemical network in all models includes 191 species linked in 8180 gas-phase as well as surface reactions. The fractional abundances (with respect to the total hydrogen in all forms) are computed in the code by the rate equation method (e.g. Cuppen et al. 2017). In this method, the chemical network of each molecule is converted into a single ordinary differential equation (ODE) that describes the time evolution of this molecule. This equation, for a species X, has the general form

$$\frac{d[X]}{dt} = \sum F(X) + D(X)$$

where $[X]$ is the concentration of the species X and $F(X)$ and $D(X)$ refers to the formation and destruction pathways of X, respectively. In order to solve the whole set of these ODEs and obtain the abundances for all the species involved in the network, we use the FORTRAN package LSODE with a double precision version (DLSODE) in which the ODEs are solved and directly integrated for all the species at each time step. The rate constants of the reactions are calculated automatically in the code using the UMIST formula (Millar et al. 1997; McElroy et al. 2013).

3 Results and discussion

In this section we represent and discuss our model results for the protostellar phase. We start with reviewing, in details, the results of the RM (Sect. 3.1), after that we discuss the effects of varying the physical conditions of the protostellar core on the chemical evolution of the deuterium chemistry (Sect. 3.2).

3.1 The reference model

Our reference model (RM) ran under the physical conditions of CMM3 listed in Table 1 after a pre-phase of a dark cloud to get the initial molecular abundances of the protostellar phase. Figure 1 represents, in the top panel, the time evolution of the molecular abundances of our model calculations, in the protostellar phase, for a selected set of deuterated species (DCO^+, N_2D^+, DCN, DNC, C_2D, and HDCO) observed in CMM3 by Watanabe et al. (2015) and their normal isotopes (XH). For each molecule, we show the time evolution of the D/H ratio with comparison with the observed value. The bottom panel of Fig. 1 is the time evolution of the set of selected deuterated molecules with some key species that derive the deuterium chemistry (D-atoms, CO, N_2, H_2D^+, CH_2D^+, and C_2HD^+). Note that the obtained increase in the abundance of some of these species is mainly due to the high CR ionisation rate in the protostellar phase (1.3 times higher than the dark cloud phase). The influence of this higher value is twofold; destruction of some gaseous species in the medium leading to an enhancement in the abundances of others such as the case of DCO^+ that is enhanced by the destruction of H_2D^+ and CH_4D^+ by CO, and releasing a small fraction of mantle species to desorb from grain surfaces to enrich the gas-phase such as the case of CO.

From Fig. 1 one may notice similarities between the evolutionary trends of hydrogenated (XH) and their deuterated counterparts (XD). This may indicate either common chemical pathway (e.g. $HCO^+ + D \rightarrow DCO^+$) or parent molecule such as ($C_2HD^+ + NH_3 \rightarrow NH_4^+ + C_2D$ or $NH_3D^+ + C_2H$). We also notice that the abundances of the species was reproducible up to a factor of 5 of the observations in particular for some XH species such as HCO^+, HCN, and HNC and their deuterated counterparts, but it was not successful in forming N_2D^+, C_2D, and HDCO and their XH isotopes. The evolutionary trends of the deuterium chemistry drivers (Fig. 1, bottom panel) and those of the studied molecules with the chemical analysis of the species may explain these results.

The chemical analysis of the RM revealed that, at any given time, the formation of N_2D^+ proceeds via the reaction of N_2 and H_2D^+ and it is destroyed by CO molecules. Since CO is very abundant in the gas ($\sim 10^{-4}$ with respect to the total H in the gas) one should expect a low abundance of H_2D^+ (e.g. Pagani et al. 2011; $< 10^{-11}$ in our RM) which could cause the less production of N_2D^+. Moreover, the high abundance of CO leads to a severe destruction of the ion with which the formation is not capable of maintaining the ion in the gas. Therefore, we barely (in the model) see the ion. The abundances of both C_2D and HDCO are comparable to those of C_2HD^+ and CH_2D^+, respectively. The chemical analysis showed that C_2D and HDCO are daughters of C_2HD^+ and CH_2D^+, respectively, and hence their low abundance is due to the shortage in the amount of their parents ($\sim 5 \times 10^{-12}$). More details on the analysis of C_2D and HDCO is discussed in Sect. 4.

DCO^+ and DCN best match observations at times (2–6) $\times 10^4$ yrs while the time of best fit of DNC is slightly later ($\sim 4 \times 10^4$ yrs) due to the lack of its parent molecules (CHD and CD_2) during earlier times. The time of best fit is within the expected age of CMM3 (Awad and Shalabeia 2017).

Although the model was not very successful in reproducing the fractional abundances of all the selected set of species, it was successful in reproducing most of the D/H ratios. The D/H ratio of HCO^+ is higher than 1 during times $< 10^4$ and it saturates at 2 after 5×10^5 yrs; when the

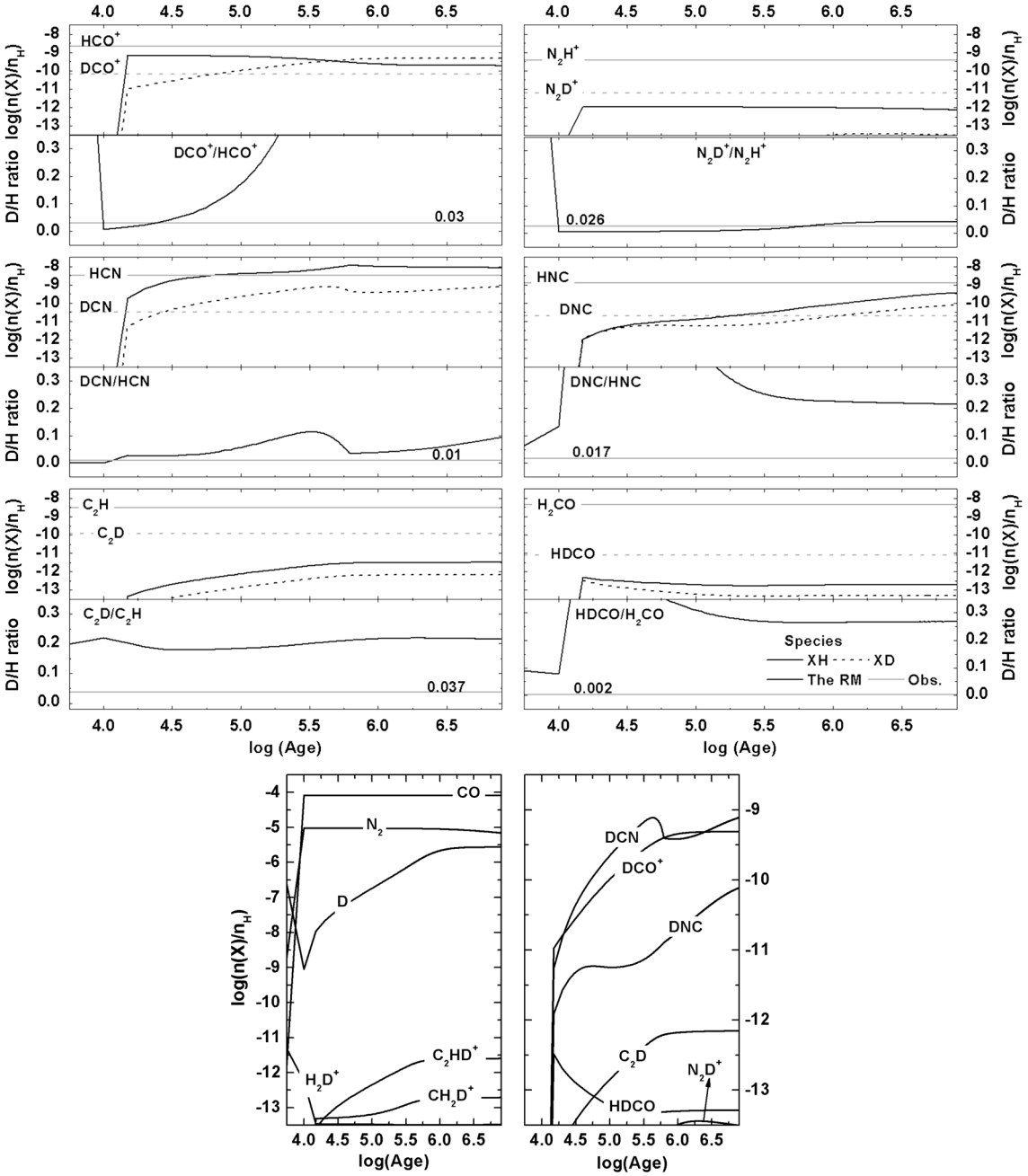

Fig. 1 *Top Panel*: abundances and D/H ratios as a function of time as calculated in the reference model (RM) of CMM3. *Solid lines* represents normal isotopes (XH) while *dashed lines* are their deuterated counterparts (XD). *Black lines* represents the model calculations and *grey ones* are observations as taken from Watanabe et al. (2015). The numbers typed in the ratio panels are the observed value. *Bottom Panel*: the time evolution of deuterated species with that of key deuterium chemistry drivers (see labels)

abundance of DCO^+ become twice that of HCO^+. The ratio of N_2H^+ also starts with values higher than unity then it declines to saturate at value comparable to observations (~ 0.03). D/H ratios > 1 are omitted because they do not have real physical meaning since most of them are obtained when the species, both or one of them, are below the detection limit ($x(X) < 10^{-13}$). When the species are detectable, we found that the ratios are in good agreement with observations during early stages, apart from those of C_2D and HDCO which are higher than observations due to their underestimated abundances.

The observed D/H ratio of H_2CO in CMM3 is ~ 10 times less than that obtained for other species. From our study, we expect that the reason for this is the low temperature of the gas (15 K) which is not enough to evaporate the species from the dust grains since formaldehyde is believed to be effec-

Table 3 Comparison between our calculated abundances and D/H ratios from the reference model (RM) and observations of selected deuterated species in NGC 2264 CMM3 from Tables 6 and 7 in Watanabe et al. (2015) at 15 K. Time of best fit, in years, is also shown in the last column

Fractional abundances				
Species	Observations†		This work	Time (in yrs)
	N(Y)	x(Y)	x(Y)	
DCO^+	7.4×10^{13}	6.5×10^{-11}	6.2×10^{-11}	$\geq 6.4 \times 10^4$
N_2D^+	7.8×10^{12}	6.8×10^{-12}	$< 1.0 \times 10^{-12}$	all times
DCN	3.6×10^{13}	3.2×10^{-11}	2.7×10^{-11}	2.4×10^4
DNC	2.4×10^{13}	2.1×10^{-11}	$\sim 1.0 \times 10^{-11}$	$> 3.8 \times 10^5$
C_2D	1.3×10^{14}	1.1×10^{-10}	$\geq 1.0 \times 10^{-12}$	all times
HDCO	1.0×10^{13}	8.8×10^{-12}	$\geq 4.0 \times 10^{-13}$	all times
D/H ratios				
The ratio	Observations		This work	Time (in yrs)
DCO^+/HCO^+	0.030 ± 0.015		0.005–0.05	$(1–4) \times 10^4$
N_2D^+/N_2H^+	0.026 ± 0.010		≤ 0.05	$\geq 1 \times 10^4$
DCN/HCN	0.010 ± 0.003		0.02–0.03	$(1–4.5) \times 10^4$
DNC/HNC	0.017 ± 0.012		> 0.05	all times
C_2D/C_2H	0.037 ± 0.032		≥ 0.2	all times
$HDCO/H_2CO$	0.002 ± 0.0015		≥ 0.1	all times

†Observed column densities, N(Y), are converted into fractional abundances with respect to H, x(Y), given the observed N(H_2) in NGC 2264 CMM3 is 5.7×10^{23} cm^{-2} (Peretto et al. 2006)

tively formed on grains (e.g. Tielens and Hagen 1982; Tielens 1983; Watanabe et al. 2003) beside its formation in the gas. Another plausible reason for this low ratio is the chemical youth of CMM3 which does not allow time for more complex organics to form given the low abundance of their deuterium initiator (C_2HD^+ and CH_2D^+). The last point is related to the sensitivity of the detector which was the argument of Watanabe et al. (2015) for not detecting multiply deuterated species as well as singly deuterated methanol. It is possible that more sensitive detectors will be able to detect more lines of H_2CO and its deuterium counterparts, and hence enhance their abundances and then improve the ratio.

A comparison between our computed abundances and the molecular D/H ratios and observations as taken from Watanabe et al. (2015) is given in Table 3.

3.2 The effect of changing the physical parameters

We investigated the impact of changing the following parameters: (1) the core density, (2) the amount of depletion onto grain surfaces, (3) the CR ionisation rate, and (4) H_2 OPR, on the fractional abundances of DCO^+, N_2D^+, DCN, DNC, C_2D, and HDCO that had been observed in CMM3 by Watanabe et al. (2015).

Generally, we find that deuterium-bearing species are affected by changes in the parameter space we explored in this study. Most of the molecular abundances are enhanced up to 400 times (e.g. models M1, M3, M4), in particular during early stages of the evolution ($t \leq 3 \times 10^4$ yrs) when compared to the results of the RM. Few evolutionary trends show similarities to those of the RM (e.g. models M2, M5, and M6) which may indicate similar pathways, but different rates. Detailed discussion of our findings is given in the following subsections. In our discussion we give the full chemical analysis of DCO^+ and DCN as an example of the ions and simple molecules, respectively, in the core.

3.2.1 The core density

In the context we are discussing the influence of changing the density of the core on the time evolution of the species understudy. Beside the reference model (RM) in which the density is 5.4×10^6 cm^{-3} (Peretto et al. 2006), we performed two models; model M1 in which the density is 5 times less than that of the RM (n_H(M1) = 1.0×10^6 cm^{-3}), and model M2 where the density (n_H(M2) = 2.0×10^7 cm^{-3}) is 5 times higher than the density of the RM. The results of these models, M1 and M2, in comparison with those of the RM are illustrated in Fig. 2. In this figure, black squares represent the RM while red circles and blue triangles denote models M1 and M2, respectively.

In general, our calculations showed that reducing the core density (model M1) enhances the abundances of most of the species up to few orders of magnitude while increasing the core density (model M2) leads to an insignificant (often less than a factor of 5) decrease in the abundances of the species, see Fig. 2. This increase in the abundances in model M1 is more pronounced during early evolutionary stages ($t \leq 3 \times 10^4$ yrs) after which the abundances converge to those of the RM at later times. The overall chemical analysis of the species in model M1 showed that their rates of formation are few orders of magnitude higher than those in the RM, in particular at $t < 10^4$ yrs, while their rates of destruction are within a factor of 5 of that calculated for the RM. Similarities between the evolutionary curves of model M2 and the RM indicate similarities in the chemical pathways, and differences in the rates of formation of species which is found to be a factor of 3–5 lower that those of the RM. Differences in the rates of formation and destruction between the three models could be attributed to differences in the abundances of the species parent molecules and their destroyers. In the following we discuss the detailed chemical analysis of DCO^+ and DCN as examples to understand how the chemistry is affected by variations in the core density. In Fig. 3 we sketch the chemical network of both DCO^+ and DCN as revealed from the RM. Additional pathways with

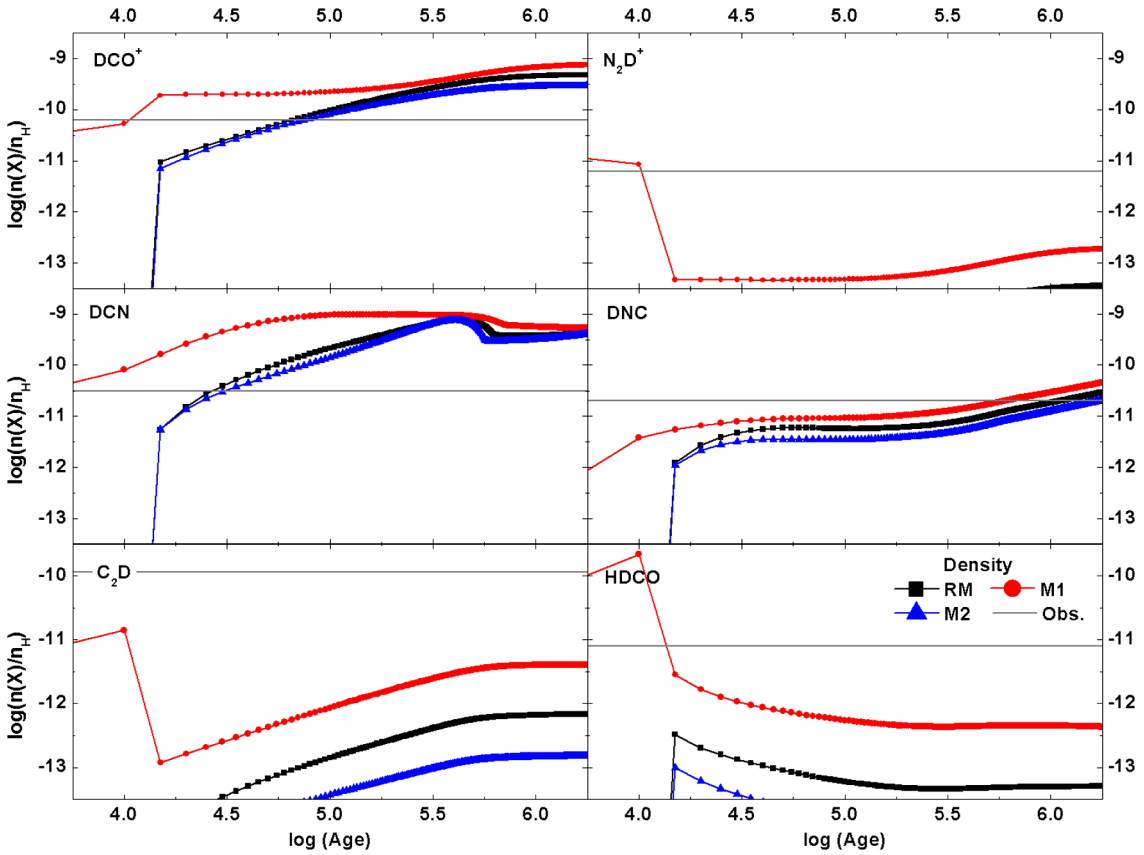

Fig. 2 Abundances as a function of time in cores with different densities; 5.4×10^6 cm^{-3} (RM, *black squares*), 1.0×10^6 cm^{-3} (M1, *red circles*) and 2.0×10^7 cm^{-3} (M2, *blue triangles*). Observed values, as taken from Watanabe et al. (2015), are represented by *solid grey line*

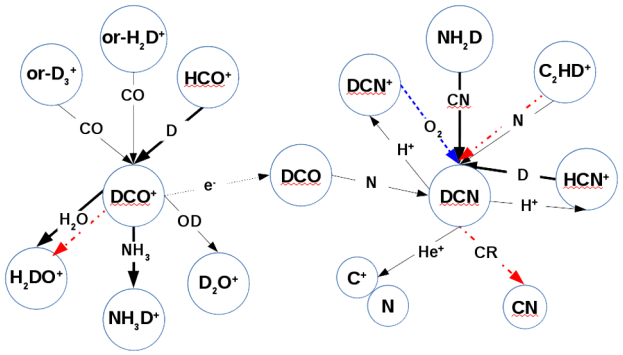

Fig. 3 The effective chemical pathways for DCO^+ and DCN in CMM3 as given by our model chemical analysis in the RM (*black arrows*), low density (*red dash-dot arrows*) and low depletion (*blue dashed line*); see text in Sect. 3. The prefix 'or-' stands for ortho

different arrow line styles indicates other routes of formation and/or destruction of the species under various physical conditions in the six models we performed.

In the RM, the formation of DCO^+ is dominated by the ion-molecule reactions of H_3^+ isotopes with CO at $t < 3 \times 10^4$ yrs, and the H-D substitution reaction '$HCO^+ + D$' at later times. The destruction of DCO^+ always occur by a competition between water (H_2O) and ammonia (NH_3). The same network is found to dominate the chemistry in models M1 and M2 with different times. The H-D substitution reaction is efficient since early stages ($t < 10^4$ yrs) giving an increase to the productivity of DCO^+ during this time interval compared to the RM and hence enhance the formation rate. At times $\geq 10^5$ yrs, the chemistry in the RM and M1 become comparable which explains the conversion of the results at late times. Moreover, the abundances of H_2O and NH_3 in the RM is higher which may also explain the lower abundance of the molecule in the RM. In denser gas (model M2), the abundances of the destroyers are slightly higher than those in the RM that in turn led to higher rates of destruction of DCO^+ (factor of 3–5 of the RM) while the comparable rates of formation could be attributed to the comparable abundances of the parent molecules in models M2 and the RM.

The same scenario is applicable for the simple molecule DCN in which its formation in the RM occurs via '$HCN^+ + D$' and '$CN + NH_2D$' and it is mainly destroyed by H^+. In model M1 the formation occur by these two routes in addition to '$DCN^+ + O_2$' at $t < 10^4$ yrs; see Fig. 3. This may increase the yield of the molecule ~ 200 times than the RM during such early stages. The fact that the abundance of

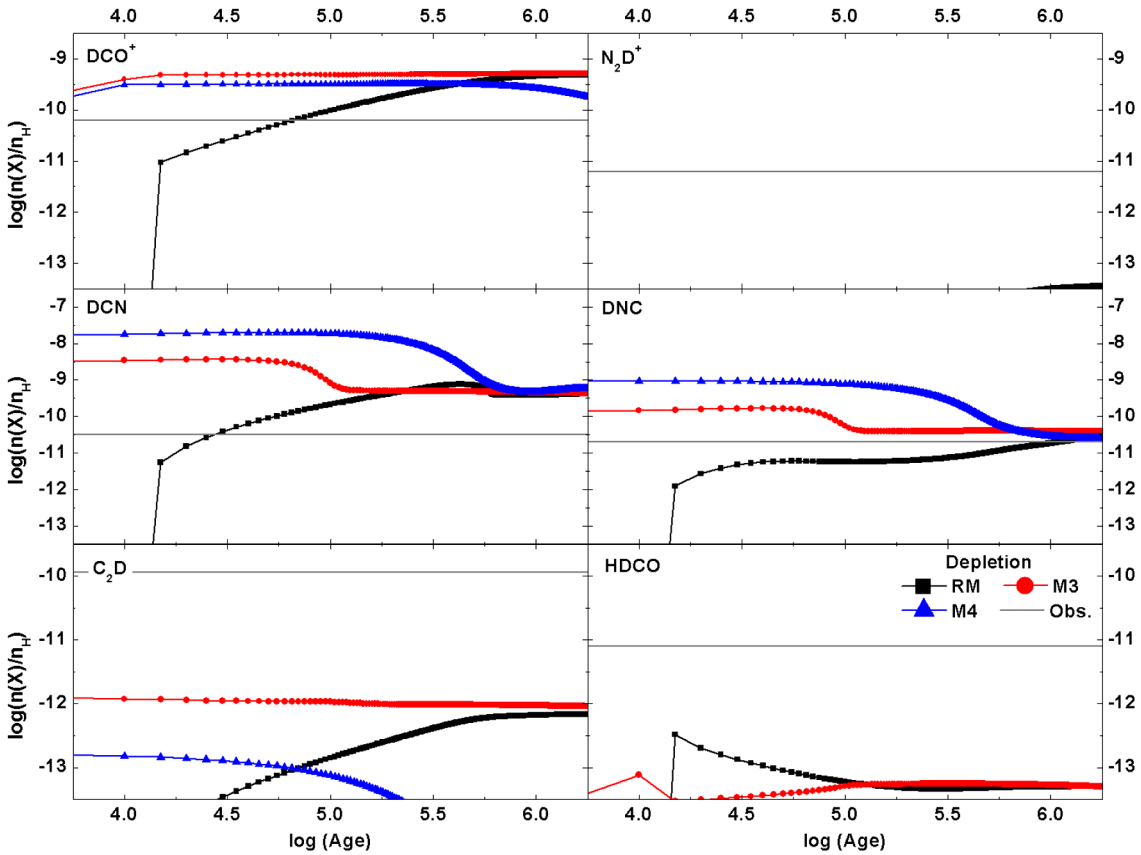

Fig. 4 The effect of varying the depletion of gaseous species onto grain surfaces on the time evolution of the calculated molecular abundances. Different curves represent different models: the RM (full depletion, *black squares*), model M3 (partial depletion, *red circles*), and model M4 (0% depletion, *blue triangles*). Observations are represented by *solid grey line* as taken from Watanabe et al. (2015)

the ion H^+, the main cause of destroying DCN, is negligible in model M1 ($\sim 10^{-11}$) compared to the RM ($\sim 10^{-8}$) during $t < 10^4$ yrs can be another reason for the high abundance of DCN during early times.

Observations of the massive protostellar core CMM3 (Saruwatari et al. 2011; Watanabe et al. 2015) suggested that the core is in its early evolutionary stages. Our results (Fig. 2) showed generally that most of the abundances of the species are in good agreement with observations in the RM at times around (1–5) $\times 10^4$ yr, except DNC which is in-line with observations at times $\geq 10^5$ yrs. These times are in agreement with the ages of protostellar objects estimated by André et al. (1993, 2000).

3.2.2 Depletion of the gas

Depletion is a measure of the amount of species removed from the gas to stick onto the grains. Therefore, changes in the depletion can be modelled by changing the sticking probability of the species onto grains (Rawlings et al. 1992). In our model, we followed this strategy in varying the depletion percentage and take the abundance of CO in the gas as the measure of the amount of depletion because it is the second most abundant gas-phase molecule after H_2 (e.g. Viti et al. 2004; Awad et al. 2010, 2014). In the following we discuss the impact of variation in the depletion percentage of gaseous material onto grain surfaces on the fractional abundances of deuterated species. The amount of gaseous species involved in surface reactions was reduced 15% of that amount in the RM in model M3 while the depletion was totally inhibited; i.e. become 0% in model M4 to simulate pure gas-phase chemistry. Figure 4 represents the time evolution of the deuterated species in CMM3 as calculated in cores with full depletion (RM, black squares), partial depletion (M3, red circles), and with no depletion (M4, blue triangles). The straight grey solid line is the observed abundance in CMM3 as taken from Watanabe et al. (2015).

When molecules are depleted onto grain surfaces, they get involved into surface reactions which enhances the abundance of their daughter molecules in the gas phase via desorption mechanisms. Therefore, by reducing the depletion onto grains we expect a general decrease in the abundances of the species because we are losing partially the contribution of surface chemistry. The results illustrated in Fig. 4 show that the sensitivity of species to depletion is differ-

ent. The abundance of DCO^+, DCN, and DNC increases in models M3 (partial depletion) and model M4 (no depletion), in particular during early stages of the evolution ($1.0 \times 10^4 < t\,(\mathrm{yr}) < 3.0 \times 10^5$) comparing to their abundances in the RM (full depletion). While the always underestimated species in our models (C_2D, HDCO, and N_2D^+) show also a respond to changes in the depletion onto grain surfaces. The abundance of N_2D^+ become invisible in both models M3 and M4, C_2D show an increase by 10 times that of the RM in both models specially at $t \leq 3 \times 10^5$ yrs, and HDCO become barely visible in M3 and invisible in M4. These results may imply a grain origin either direct or indirect of these three species. It is remarkable that the abundances of these species either in models M3 or M4 always overestimate their observed values.

The detailed analysis of the species DCO^+ and DCN showed that the main reason for their enhancement is the increase in their production rates in models M3 and M4 than that in the RM specially at early times. The reduction of the amount of species freezes onto grains increases their amount in the gas-phase allowing longer stay of the parent molecules in the region and hence more final products. In the case of DCN, the chemical analysis revealed a different chemistry at work in models M3 and M4 compared to the RM (Fig. 3). The molecule is formed mainly by '$C_2HD^+ + N$' and the destruction in M3 happens by He^+ which is not as effective as H^+ in the RM which leads to more DCN in the core in model M3. In model M4, CR dissociation reactions are the main destruction routes of DCN, but also they are not as efficient as the destruction by H^+ in the RM so more DCN stayed in the gas.

We found that the case of N_2D^+ is interesting because it does not show an enhancement in its abundance in contrary to other ions in the core. The analysis of this species showed that the ion N_2D^+ is formed in the gas-phase in the RM mainly by the reaction '$orH_2D^+ + N_2$' which become less efficient in model M3 and the formation took place via the deuterium exchange with N_2H^+, but with a formation rate 15 times less than that in the RM. In addition, the destruction of the ion by CO molecules become more efficient in model M3, 30 times higher than that in the RM because the abundance of CO in the former model is 15–20 times higher than the RM.

The increase in the amount of the deuterated species in partially depleted cores is in-line with observations of cold dense core (Bacmann et al. 2003), however these models (M3 and M4) cannot reproduce observations of CMM3 by Watanabe et al. (2015). Thus we conclude that deuterated species are formed in fully depleted cores.

3.2.3 The CR ionisation rate

CR ionisation reactions are of special importance because they are the driver of the interstellar gas-phase chemistry since they are the main route of the formation of H_3^+ ions. When these ions react with HD molecules they form H_2D^+ which leads the interstellar deuterium gas chemistry (Millar et al. 1989; Millar 2005). For this reason, we studied the influence of changing the CR ionisation rate, ζ, on the abundances of deuterated species in the core. Several observations (e.g. van der Tak and van Dishoeck 2000; Doty et al. 2002; Morales Ortiz et al. 2014; Kaźmierczak-Barthel et al. 2015) measured this rate in massive protostars and found it to be up to 500 times the standard interstellar value ($\zeta_{\mathrm{ISM}} = 1.3 \times 10^{-17}\ \mathrm{s}^{-1}$; Lepp 1992) with a preferred range (5–10)ζ_{ISM}. Most recently, Awad and Shalabeia (2017) calculated this rate (theoretically) for the massive protostellar core CMM3 and found that $\zeta_{\mathrm{CMM3}} = 1.3\zeta_{\mathrm{ISM}}$. In order to understand this influence in CMM3, we ran two models with higher ionisation rates than the RM; model M5 ($\zeta_{\mathrm{CMM3}} = 5\zeta_{\mathrm{ISM}}$) and model M6 ($\zeta_{\mathrm{CMM3}} = 10\zeta_{\mathrm{ISM}}$), see Table 2. The model results in comparison with the RM are illustrated in Fig. 5 in which results of models M5 and M6 are represented by red circles and blue triangles, respectively. From the figure, we notice that evolutionary trends show similarities to those obtained in the RM (black squares) but with higher abundances. The increase in the abundance is directly proportional to the increase in the ionisation rate.

The chemical analysis of DCO^+ in models M5 and M6 showed similarities to that of the RM, as indicated by solid arrows in Fig. 3. The formation of DCO^+ occurs by the reaction '$orH_2D^+ + CO$', at times $t \leq 10^4$ yrs, and the reaction '$HCO^+ + D$', for $t > 10^4$ yrs. The enhancement of the CR ionisation rate enriches the medium with ions and hence increases the ultimate amount of DCO^+ (Fig. 3). The simple molecule DCN is formed in models M5 and M6 by through the same route in the RM. Enhancing the CR ionisation rate, allow more dissociation reactions in the medium and enhanced the amount of radicals. This opened a new path for the production of the molecule which is '$N + CHD$' which increased the amount of DCN in the medium.

It is noticeable that the results of models M5 and the RM are better match to observations than model M6 (blue line). From this we may conclude that the CR ionisation rate, ζ, in the CMM3 is ranged between 1.3–5ζ_{ISM}. This result is in-line with both observations (van der Tak and van Dishoeck 2000) and previous models of CMM3 (Awad and Shalabeia 2017).

3.2.4 H_2 OPR

We ran few models similar in the physical conditions to the RM, but with different initial H_2 OPR; following the work by Pagani et al. (2011). We found that in the protostellar phase, the focus of this work, variations in the OPR do not affect the fractional abundances of deuterated species and hence their D/H ratio. On the other hand, deuterium chemistry found to be mostly affected by changes in the H_2 OPR

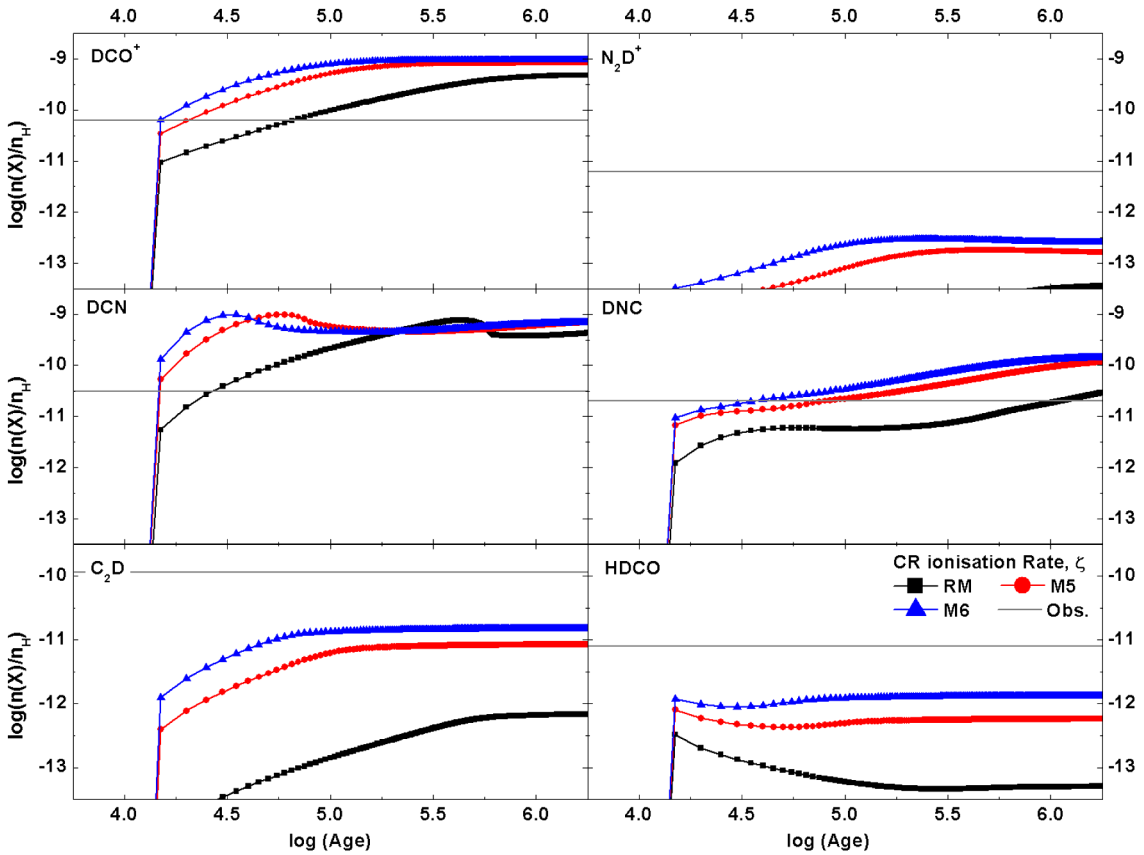

Fig. 5 The chemical evolution of deuterated species as a function of time in cores with different CR ionisation rates, ζ. The RM ($1.3\zeta_{\rm ISM}$, *black squares*), model M5 ($5\zeta_{\rm ISM}$, *red circles*) and model M6 ($10\zeta_{\rm ISM}$, *blue triangles*). Observed values, as taken from Watanabe et al. (2015), are represented by *solid grey line*

during the dark cloud stage, which is the stage prior to the formation of the protostar. The chemical analysis of this dark cloud phase revealed that the abundances of deuterated species are enhanced by factors up to 10 when the OPR goes below 0.1, in particular for DCO^+ and N_2D^+. The chemistry of these two species is based on the abundances of the isotopologues of H_3^+ by their reactions with CO and N_2, respectively. The other studied molecules (DCN, DNC, C_2D, HDCO) do not show a significant change (factor < 5) in their abundances with OPR because their main formation routes depends on CH_2D^+ and C_2HD^+ which are independent on OPR. In addition, these latter deuterium chemistry drivers are more important in regions with $T \geq 30$ K (Millar et al. 1989). In the protostellar phase and since the beginning of the chemistry, species tend to converge to values obtained in the RM and variations in the OPR do not have any influence on their abundances in particular at times $\geq 10^4$ years when they become detectable. The reason for this might be the higher CR ionisation rate in CMM3 when compared to the dark cloud that in turn leads to destruction of the species during the very early times of the protostar. A comprehensive study on this topic and more observations may help for better understanding.

4 Model limitations

Although our results for the performed models match observations for DCO^+, DCN and DNC at times $\leq 10^5$ yrs, under different physical conditions, all of our models failed in reproducing the observed amount of both C_2D and HDCO under any circumstances.

The formation pathway of C_2D, as unveiled from the analysis of the RM, occurs in the gas-phase through the reaction of NH_3 with C_2HD^+ where the latter molecule is formed mainly by either reactions '$HD + C_2H_2$' or '$C^+ + CH_3D$'. The second pathway via deuterated methane (CH_3D) dominates the chemistry at times $> 10^3$ yrs. Given the low temperature of the gas in CMM3 (15 K) and that the sublimation temperature of CH_4 ices is ~ 30 K, the abundance of the reactants CH_3D and, therefore, C_2HD^+ will be very low and cannot account for the formation of larger amounts of C_2D. Another important point is that the deuterium enrichment via C_2HD^+ occurs in warm media (Millar et al. 1989), and hence the efficiency of deuteration for this molecule is going to be low.

On the other hand, the formation of HDCO takes place both in the gas and on grain surfaces in which it is believed

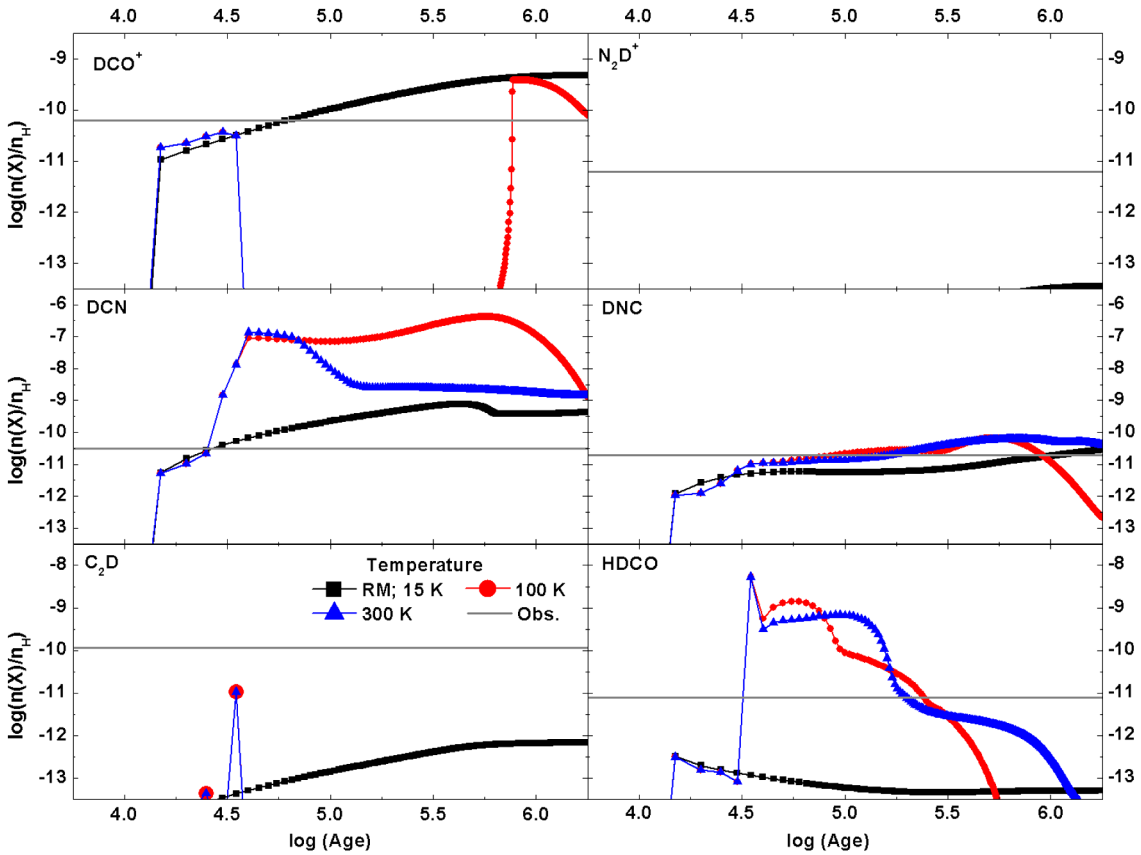

Fig. 6 The chemical evolution of deuterated species as a function of time under higher temperatures $T = 100$ K (*red circles*), and 300 K (*blue triangles*) in comparison with the RM at 15 K (*black squares*). Observed values, as taken from Watanabe et al. (2015), are represented by *solid grey line*

that the efficiency of mantle production is higher (Tielens 1983; Watanabe and Kouchi 2008). In the gas-phase, HDCO formation is based on the molecule C_2HD and CHD where both are daughters of CH_2D^+ and C_2HD^+. These two parents have low abundances in the gas, as calculated in our RM, (see bottom panel in Fig. 1) leading to the low obtained abundance of HDCO.

There is a possibility that HDCO and C_2D are formed in warmer regions (e.g. hot core; $\geq$ 100 K), rather than the cold (15 K) protostellar core observed by Watanabe et al. (2015). In order to test this possibility, we ran a hot core model using the physical parameters of the protostellar core of CMM3, but at higher temperatures of 100 K and 300 K; see Fig. 6. The results of both models show that C_2D is enhanced at times correspond to the temperature range 70–90 K then it declines and become undetectable. The model calculations still underestimate the abundance of C_2D. The analysis showed that the decrease in C_2D abundance at times $t > 31{,}000$ yrs is mainly due to (i) its destruction by gaseous O_2, and (ii) the destruction of its parent molecule, C_2HD^+, by para-H_2 which are very abundant in the core. On the contrary, the abundance of HDCO increases and exceeds the observed value, at times when $T \geq 100$ K (for both models) due to its sublimation from grains. Surprisingly, DNC showed a better agreement with observations at the hot core temperatures. These results may imply that HDCO and DNC may be formed in warmer areas than the other species and could be used as tracers of these hot core regions while models should consider another mechanism to account for warm carbon-chain molecules (e.g. C_2D) which is formed in warm gas but not necessarily in the hot core.

The amount of mantle C_2D and HDCO molecules are found to be comparable to their observed gaseous values by Watanabe et al. (2015). This may lead to another limitation of the model, if these species are not formed in hot cores, which is the limited number of desorption mechanisms we use in our model at low temperatures. At the moment, we are working on including more non-thermal desorption mechanisms such as chemical explosions and sputtering which are important specially in dense regions. In addition, Saruwatari et al. (2011) suggested that the core CMM3 might be exposed to or affected by slow shocks from its surrounding region. We are also considering studying the influence of including shocks on the chemistry of the region (Awad et al. in preparation).

5 Conclusions

We studied the sensitivity of deuterium chemistry in the massive young protostellar core NGC 2264 CMM3 to its surrounding physical conditions by running gas-grain chemical models. We summarise our conclusions as follows:

1. In CMM3, the deuterium chemistry is sensitive to changes in the core density, depletion percentage, and the CR ionisation rate. Therefore, we cannot use any of these studied molecules as a tracer to the physics of the region.
2. Deuterium chemistry is insensitive to changes in the H_2 OPR under the physical conditions of prestellar objects, but it is very sensitive to these variations in the pre-stage of dark clouds.
3. The model reproduces observations for cores with density range (1–5) $\times 10^6$ cm^{-3} or CR ionisation rate between (1.69 and 6.5) $\times 10^{-17}$ s^{-1}.
4. Time of best fit with observations ($t < 10^5$ yrs) is in-line with the estimated age of young protostellar cores (André et al. 1993, 2000). We then confirms that CMM3 is in its early evolutionary stage and its estimated age is (1–5) $\times 10^4$ yrs.
5. HDCO and DNC might be formed in hot cores rather than the cold protostellar region and hence they may trace hotter gas (> 100 K) while the formation of C_2D is linked to warm deuterium chemistry, but they are not necessarily trace the hot core region.

Acknowledgement The authors would like to thank the referee for the valuable comments that helped in improving the original manuscript.

References

Aikawa, Y., Wakelam, V., Hersant, F., Garrod, R.T., Herbst, E.: Astrophys. J. **760**, 40 (2012). 1210.2476. https://doi.org/10.1088/0004-637X/760/1/40

Albertsson, T., Semenov, D.A., Vasyunin, A.I., Henning, T., Herbst, E.: Astrophys. J. Suppl. Ser. **207**, 27 (2013). https://doi.org/10.1088/0067-0049/207/2/27

André, P., Ward-Thompson, D., Barsony, M.: Astrophys. J. **406**, 122 (1993). https://doi.org/10.1086/172425

André, P., Ward-Thompson, D., Barsony, M.: In: Protostars and Planets IV, p. 59 (2000). arXiv:astro-ph/9903284

Asplund, M., Grevesse, N., Sauval, A.J., Scott, P.: Annu. Rev. Astron. Astrophys. **47**, 481 (2009). 0909.0948. https://doi.org/10.1146/annurev.astro.46.060407.145222

Awad, Z., Shalabeia, O.M.: Astrophys. Space Sci. **362**, 83 (2017). 1703.04632. https://doi.org/10.1007/s10509-017-3061-8

Awad, Z., Viti, S., Collings, M.P., Williams, D.A.: Mon. Not. R. Astron. Soc. **407**, 2511 (2010). 1005.5265. https://doi.org/10.1111/j.1365-2966.2010.17077.x

Awad, Z., Viti, S., Bayet, E., Caselli, P.: Mon. Not. R. Astron. Soc. **443**, 275 (2014). 1406.2272. https://doi.org/10.1093/mnras/stu1141

Bacmann, A., Lefloch, B., Ceccarelli, C., Steinacker, J., Castets, A., Loinard, L.: Astrophys. J. Lett. **585**, 55 (2003). arXiv:astro-ph/0301651. https://doi.org/10.1086/374263

Bergman, P., Parise, B., Liseau, R., Larsson, B.: Astron. Astrophys. **527**, 39 (2011). 1011.3339. https://doi.org/10.1051/0004-6361/201015012

Brown, P.D., Millar, T.J.: Mon. Not. R. Astron. Soc. **240**, 25 (1989a)

Brown, P.D., Millar, T.J.: Mon. Not. R. Astron. Soc. **237**, 661 (1989b)

Caselli, P., Ceccarelli, C.: Astron. Astrophys. Rev. **20**, 56 (2012). 1210.6368. https://doi.org/10.1007/s00159-012-0056-x

Ceccarelli, C., Loinard, L., Castets, A., Tielens, A.G.G.M., Caux, E., Lefloch, B., Vastel, C.: Astron. Astrophys. **372**, 998 (2001). https://doi.org/10.1051/0004-6361:20010559

Ceccarelli, C., Caselli, P., Herbst, E., Tielens, A.G.G.M., Caux, E.: In: Reipurth, B., Jewitt, D., Keil, K. (eds.) Protostars and Planets V, p. 47 (2007)

Coutens, A., Vastel, C., Cazaux, S., Bottinelli, S., Caux, E., Ceccarelli, C., Demyk, K., Taquet, V., Wakelam, V.: Astron. Astrophys. **553**, 75 (2013). 1304.2890. https://doi.org/10.1051/0004-6361/201220967

Coutens, A., Vastel, C., Hincelin, U., Herbst, E., Lis, D.C., Chavarría, L., Gérin, M., van der Tak, F.F.S., Persson, C.M., Goldsmith, P.F., Caux, E.: Mon. Not. R. Astron. Soc. **445**, 1299 (2014). 1409.1092. https://doi.org/10.1093/mnras/stu1816

Crapsi, A., Caselli, P., Walmsley, C.M., Myers, P.C., Tafalla, M., Lee, C.W., Bourke, T.L.: Astrophys. J. **619**, 379 (2005). arXiv:astro-ph/0409529. https://doi.org/10.1086/426472

Cuppen, H.M., Walsh, C., Lamberts, T., Semenov, D., Garrod, R.T., Penteado, E.M., Ioppolo, S.: Space Sci. Rev. **212**, 1 (2017). https://doi.org/10.1007/s11214-016-0319-3

Doty, S.D., van Dishoeck, E.F., van der Tak, F.F.S., Boonman, A.M.S.: Astron. Astrophys. **389**, 446 (2002). astro-ph/0205292. https://doi.org/10.1051/0004-6361:20020597

Flower, D.R., Pineau Des Forêts, G., Walmsley, C.M.: Astron. Astrophys. **449**, 621 (2006). arXiv:astro-ph/0601429. https://doi.org/10.1051/0004-6361:20054246

Furuya, K., van Dishoeck, E.F., Aikawa, Y.: Astron. Astrophys. **586**, 127 (2016). 1512.04291. https://doi.org/10.1051/0004-6361/201527579

Furuya, K., Aikawa, Y., Nomura, H., Hersant, F., Wakelam, V.: Astrophys. J. **779**, 11 (2013). 1310.3342. https://doi.org/10.1088/0004-637X/779/1/11

Gerlich, D., Herbst, E., Roueff, E.: Planet. Space Sci. **50**, 1275 (2002). https://doi.org/10.1016/S0032-0633(02)00094-6

Herbst, E., van Dishoeck, E.F.: Annu. Rev. Astron. Astrophys. **47**, 427 (2009). https://doi.org/10.1146/annurev-astro-082708-101654

Hincelin, U., Herbst, E., Chang, Q., Vasyunina, T., Aikawa, Y., Furuya, K.: In: 69th International Symposium on Molecular Spectroscopy, p. 9 (2014)

Huang, J., Öberg, K.I.: Astrophys. J. Lett. **809**, 26 (2015). 1508.03637. https://doi.org/10.1088/2041-8205/809/2/L26

Kaźmierczak-Barthel, M., Semenov, D.A., van der Tak, F.F.S., Chavarría, L., van der Wiel, M.H.D.: Astron. Astrophys. **574**, 71 (2015). 1412.5763. https://doi.org/10.1051/0004-6361/201424657

Lepp, S.: In: Singh, P.D. (ed.) Astrochemistry of Cosmic Phenomena. IAU Symposium, vol. 150, p. 471 (1992)

Loinard, L., Castets, A., Ceccarelli, C., Caux, E., Tielens, A.G.G.M.: Astrophys. J. Lett. **552**, 163 (2001). https://doi.org/10.1086/320331

Loren, R.B., Wootten, A.: Astrophys. J. **299**, 947 (1985). https://doi.org/10.1086/163761

Majumdar, L., Gratier, P., Ruaud, M., Wakelam, V., Vastel, C., Sipilä, O., Hersant, F., Dutrey, A., Guilloteau, S.: Mon. Not. R. Astron. Soc. **466**, 4470 (2017). 1612.07845. https://doi.org/10.1093/mnras/stw3360

Maury, A.J., André, P., Li, Z.-Y.: Astron. Astrophys. **499**, 175 (2009). 0902.1379. https://doi.org/10.1051/0004-6361/200811442

McElroy, D., Walsh, C., Markwick, A.J., Cordiner, M.A., Smith, K., Millar, T.J.: Astron. Astrophys. **550**, 36 (2013). 1212.6362. https://doi.org/10.1051/0004-6361/201220465
Miettinen, O., Harju, J., Haikala, L.K., Juvela, M.: Astron. Astrophys. **538**, 137 (2012). 1112.5053. https://doi.org/10.1051/0004-6361/201117849
Millar, T.J.: Astron. Geophys. **46**(2), 020000 (2005). https://doi.org/10.1111/j.1468-4004.2005.46229.x
Millar, T.J., Bennett, A., Herbst, E.: Astrophys. J. **340**, 906 (1989). https://doi.org/10.1086/167444
Millar, T.J., Farquhar, P.R.A., Willacy, K.: Astron. Astrophys. Suppl. Ser. **121**, 139 (1997). https://doi.org/10.1051/aas:1997118
Morales Ortiz, J.L., Ceccarelli, C., Lis, D.C., Olmi, L., Plume, R., Schilke, P.: Astron. Astrophys. **563**, 127 (2014). 1306.3012. https://doi.org/10.1051/0004-6361/201322071
Öberg, K.I., Furuya, K., Loomis, R., Aikawa, Y., Andrews, S.M., Qi, C., van Dishoeck, E.F., Wilner, D.J.: Astrophys. J. **810**, 112 (2015). 1508.07296. https://doi.org/10.1088/0004-637X/810/2/112
Oliveira, C.M., Hébrard, G., Howk, J.C., Kruk, J.W., Chayer, P., Moos, H.W.: Astrophys. J. **587**, 235 (2003). arXiv:astro-ph/0212506. https://doi.org/10.1086/368019
Pagani, L., Roueff, E., Lesaffre, P.: Astrophys. J. Lett. **739**, 35 (2011). 1109.6495. https://doi.org/10.1088/2041-8205/739/2/L35
Peretto, N., André, P., Belloche, A.: Astron. Astrophys. **445**, 979 (2006). astro-ph/0508619. https://doi.org/10.1051/0004-6361:20053324
Peretto, N., Hennebelle, P., André, P.: Astron. Astrophys. **464**, 983 (2007). astro-ph/0611277. https://doi.org/10.1051/0004-6361:20065653
Rawlings, J.M.C., Hartquist, T.W., Menten, K.M., Williams, D.A.: Mon. Not. R. Astron. Soc. **255**, 471 (1992)
Roberts, H., Millar, T.J.: Astron. Astrophys. **364**, 780 (2000a)
Roberts, H., Millar, T.J.: Astron. Astrophys. **361**, 388 (2000b)
Roberts, H., Herbst, E., Millar, T.J.: Astrophys. J. Lett. **591**, 41 (2003). https://doi.org/10.1086/376962
Roberts, H., Herbst, E., Millar, T.J.: Astron. Astrophys. **424**, 905 (2004). https://doi.org/10.1051/0004-6361:20040441
Roberts, J.F., Rawlings, J.M.C., Viti, S., Williams, D.A.: Mon. Not. R. Astron. Soc. **382**, 733 (2007). 0708.3374. https://doi.org/10.1111/j.1365-2966.2007.12402.x
Rodgers, S.D., Millar, T.J.: Mon. Not. R. Astron. Soc. **280**, 1046 (1996)
Sakai, N., Sakai, T., Yamamoto, S.: Astrophys. J. **660**, 363 (2007). https://doi.org/10.1086/512774
Sakai, N., Sakai, T., Hirota, T., Yamamoto, S.: Astrophys. J. **702**, 1025 (2009). https://doi.org/10.1088/0004-637X/702/2/1025
Saruwatari, O., Sakai, N., Liu, S.-Y., Su, Y.-N., Sakai, T., Yamamoto, S.: Astrophys. J. **729**, 147 (2011). https://doi.org/10.1088/0004-637X/729/2/147
Sipilä, O., Hugo, E., Harju, J., Asvany, O., Juvela, M., Schlemmer, S.: Astron. Astrophys. **509**, 98 (2010). 0911.1236. https://doi.org/10.1051/0004-6361/200913350
Snow, T.P., McCall, B.J.: Annu. Rev. Astron. Astrophys. **44**, 367 (2006). https://doi.org/10.1146/annurev.astro.43.072103.150624
Tielens, A.G.G.M.: Astron. Astrophys. **119**, 177 (1983)
Tielens, A.G.G.M.: Rev. Mod. Phys. **85**, 1021 (2013). https://doi.org/10.1103/RevModPhys.85.1021
Tielens, A.G.G.M., Hagen, W.: Astron. Astrophys. **114**, 245 (1982)
Tiné, S., Roueff, E., Falgarone, E., Gerin, M., Pineau des Forêts, G.: Astron. Astrophys. **356**, 1039 (2000)
van der Tak, F.F.S., van Dishoeck, E.F.: Astron. Astrophys. **358**, 79 (2000). astro-ph/0006246
van der Tak, F.F.S., Müller, H.S.P., Harding, M.E., Gauss, J.: Astron. Astrophys. **507**, 347 (2009). 0909.0390. https://doi.org/10.1051/0004-6361/200912912
van Dishoeck, E.F., Thi, W.-F., van Zadelhoff, G.-J.: Astron. Astrophys. **400**, 1 (2003). arXiv:astro-ph/0301571. https://doi.org/10.1051/0004-6361:20030091
van Dishoeck, E.F., Blake, G.A., Jansen, D.J., Groesbeck, T.D.: Astrophys. J. **447**, 760 (1995). https://doi.org/10.1086/175915
Vastel, C., Mookerjea, B., Pety, J., Gerin, M.: Astron. Astrophys. **597**, 45 (2017). 1611.07389. https://doi.org/10.1051/0004-6361/201629289
Viti, S., Collings, M.P., Dever, J.W., McCoustra, M.R.S., Williams, D.A.: Mon. Not. R. Astron. Soc. **354**, 1141 (2004). arXiv:astro-ph/0406054. https://doi.org/10.1111/j.1365-2966.2004.08273.x
Wakelam, V., Loison, J.-C., Herbst, E., Pavone, B., Bergeat, A., Béroff, K., Chabot, M., Faure, A., Galli, D., Geppert, W.D., Gerlich, D., Gratier, P., Harada, N., Hickson, K.M., Honvault, P., Klippenstein, S.J., Le Picard, S.D., Nyman, G., Ruaud, M., Schlemmer, S., Sims, I.R., Talbi, D., Tennyson, J., Wester, R.: Astrophys. J. Suppl. Ser. **217**, 20 (2015). 1503.01594. https://doi.org/10.1088/0067-0049/217/2/20
Walmsley, C.M., Flower, D.R., Pineau des Forêts, G.: Astron. Astrophys. **418**, 1035 (2004). arXiv:astro-ph/0402493. https://doi.org/10.1051/0004-6361:20035718
Ward-Thompson, D., Zylka, R., Mezger, P.G., Sievers, A.W.: Astron. Astrophys. **355**, 1122 (2000)
Watanabe, N., Kouchi, A.: Prog. Surf. Sci. **83**, 439 (2008)
Watanabe, N., Shiraki, T., Kouchi, A.: Astrophys. J. Lett. **588**, 121 (2003). https://doi.org/10.1086/375634
Watanabe, Y., Sakai, N., López-Sepulcre, A., Furuya, R., Sakai, T., Hirota, T., Liu, S.-Y., Su, Y.-N., Yamamoto, S.: Astrophys. J. **809**, 162 (2015). 1507.04958. https://doi.org/10.1088/0004-637X/809/2/162
Watson, W.D.: In: Les Spectres des Molécules Simples au Laboratoire et en Astrophysique, p. 526 (1980)